

Abnormal temperature dependence of interband electronic transitions in relaxor-based ferroelectric $(1-x)\text{Pb}(\text{Mg}_{1/3}\text{Nb}_{2/3})\text{O}_3-x\text{PbTiO}_3$ ($x=0.24$ and 0.31) single crystals

J. J. Zhu (诸佳俊),¹ W. W. Li (李文武),¹ G. S. Xu (许桂生),² K. Jiang (姜凯),¹
Z. G. Hu (胡志高),^{1,a)} M. Zhu (朱敏),³ and J. H. Chu (褚君浩)¹

¹Key Laboratory of Polar Materials and Devices, Ministry of Education, Department of Electronic Engineering, East China Normal University, Shanghai 200241, People's Republic of China

²R&D Center of Synthetic Crystals, Shanghai Institute of Ceramics, Chinese Academy of Sciences, Shanghai 201800, People's Republic of China

³Department of Physics, Shanghai Jiao Tong University, Shanghai 200240, People's Republic of China

(Received 17 November 2010; accepted 9 February 2011; published online 3 March 2011)

The transmittance spectra of $(1-x)\text{Pb}(\text{Mg}_{1/3}\text{Nb}_{2/3})\text{O}_3-x\text{PbTiO}_3$ ($x=0.24$ and 0.31) single crystals have been studied in the temperature range of 5.3–300 K. It was found that the direct band gap E_{gd} is 3.150 ± 0.016 eV, indirect band gap E_{gi} is 2.939 ± 0.014 eV, and the phonon energy E_p is 0.098 ± 0.014 eV for the PMN-0.24PT crystal at 300 K. With increasing the temperature, the E_{gd} of the PMN-0.24PT crystal decreases from 3.263 ± 0.017 to 3.150 ± 0.016 eV while the E_{gd} of the PMN-0.31PT crystal increases from 3.050 ± 0.015 to 3.101 ± 0.016 eV. The peculiar characteristic can be ascribed to the monoclinic and rhombohedral multiphase coexistence in the PMN-0.31PT crystal. © 2011 American Institute of Physics. [doi:10.1063/1.3560342]

Ferroelectric (FE) materials have recently attracted considerable attention and intensive research due to their unique advantages in nonvolatile random-access memories, electro-optic devices, pyroelectric detectors, and optical mixers.^{1–5} In particular, Pb-based perovskite FE materials, such as PbTiO_3 (PT), $\text{Pb}(\text{Zr}_{1-x}\text{Ti}_x)\text{O}_3$ (PZT), $\text{Pb}(\text{Zn}_{1/3}\text{Nb}_{2/3})\text{O}_3-x\text{PbTiO}_3$ (PZN-PT), $\text{Pb}(\text{Mg}_{1/3}\text{Nb}_{2/3})\text{O}_3$ (PMN), $\text{Pb}(\text{Mg}_{1/3}\text{Nb}_{2/3})\text{O}_3-x\text{PbTiO}_3$ (PMN-PT) have been widely studied because of the potential advantages for electro-optic and microelectronic applications. Among these materials, relaxor perovskite PMN-PT single crystal is a very promising compound as the candidate of FE material for electromechanical transducers due to its excellent piezoelectric coefficients d_{33} , ultrahigh strain levels with low hysteresis, high dielectric constant, large electro-optic coefficients, and large electromechanical coupling factor k_{33} .¹ Physical properties of PMN-PT are sensitive to Ti content, poling strength, crystallographic orientation.^{6,7} The structure of PMN-PT contains the coexistence of neighboring phases in a broad composition range near the morphotropic phase boundary (MPB).^{8–10} Although the dielectric permittivity, domain structure, hysteresis loop, and piezoelectric have been widely investigated,^{6–10} the reports on electronic transitions of PMN-PT are still scarce.

On the other hand, the investigations on PMN-PT crystals at low temperature have been mainly focused on the phase transition behavior and domain structures.^{11,12} Up to date, less attention has been paid to the optical properties, especially the temperature dependence of electronic structures for PMN-PT materials. As we know, transmittance spectra can provide optical band gap (OBG), optical constants, absorption characteristics, band tail state behavior, and optical phonon modes.^{7,12} In this letter, we present the temperature dependence of fundamental optical transition in

$(1-x)\text{Pb}(\text{Mg}_{1/3}\text{Nb}_{2/3})\text{O}_3-x\text{PbTiO}_3$ ($x=0.24$ and 0.31) single crystals.

The PMN-PT single crystals were prepared by a modified Bridgman technique.³ The samples were cut perpendicular to the $\langle 001 \rangle$ direction and the thicknesses were about 0.37 mm. The crystallinity of the PMN-PT crystals were examined by the x-ray diffraction (XRD) with $\text{Cu } K\alpha$ radiation (D/MAX-2550 V, Rigaku Co.) at room temperature. Raman spectra were collected by a micro-Raman spectrometer. The normal-incident transmittance spectra were measured by a double beam ultraviolet-infrared spectrophotometer (PerkinElmer UV/VIS Lambda 950) at the photon energy of 2650–190 nm (0.5–6.5 eV) with the interval of 2 nm. The samples were mounted on a cold stage of an optical cryostat (Janis SHI-4-1) and capable of cooling from 300 to 5.3 K.

As shown in the inset of Fig. 1(a) and Fig 2(a), the crystals are found to be the rhombohedral phase for the PMN-0.24PT crystal and two-phase mixture of monoclinic and rhombohedral phases for the PMN-0.31PT crystal. The coexistence of neighboring phases in/near the MPB region is due to a first-order phase transition.^{8,11} Similar phenomena were also been observed in PZT, PMN-0.3PT, PMN-0.4PT, $0.92\text{Pb}(\text{Fe}_{1/2}\text{Nb}_{1/2})\text{O}_3-0.08\text{PbTiO}_3$, and PZN-0.07PT.^{11–16} Note that the PMN-0.4PT is mixed with the tetragonal and monoclinic phases while the present PMN-0.31PT has the coexistence of the rhombohedral and monoclinic phases.¹² This is because the PMN-PT solid solutions have a MPB near $x \sim 0.33$, dividing the rhombohedral phase and the tetragonal one. Rietveld analysis of the XRD data reveals that the phase in the present PMN-0.31PT is more likely monoclinic (M_C type) with Pm space group instead of monoclinic (M_B type) with Cm space group.⁸ It is different from the monoclinic phase of Cm (M_A type) in PZT, similar to that of space group Pm (M_C type) in PZN-PT.^{13,17} Note that the monoclinic phases with space group Cm and Pm are associated with the composition of PT in the PMN-PT crystal.⁸

^{a)}Author to whom correspondence should be addressed. Electronic mail: zghu@ee.ecnu.edu.cn. Tel.: +86-21-54345150. FAX: +86-21-54345119.

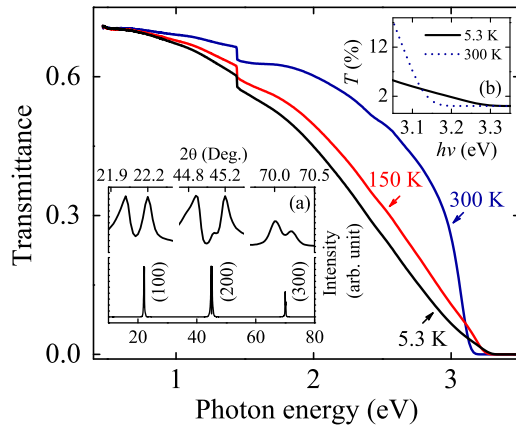


FIG. 1. (Color online) Transmittance spectra for the $\text{Pb}(\text{Mg}_{1/3}\text{Nb}_{2/3})\text{O}_3 - 0.24\text{PbTiO}_3$ (PMN-0.24PT) single crystal at the temperatures of 5.3 K, 150 K, and 300 K, respectively. The discontinuities of all the experimental data at 1.44 eV are due to the change in monochromator. The inset (a) shows XRD pattern of the PMN-0.24PT single crystal at room temperature. The inset (b) shows the transmittance spectra at temperatures of 5.3 and 300 K near the direct band gap.

Figures 1 and 2 show that the transmittance spectra of the PMN-0.31PT and PMN-0.24PT crystal. The latter has an obvious intersection point in the vicinity of the absorption edges, as seen in the inset (b) of Fig. 1. Interestingly, the absorption edge of the PMN-0.24PT crystal has a blueshift trend with decreasing the temperature while that of the PMN-0.31PT crystal presents the redshift variation. In $\text{A}(\text{B}_1\text{B}_2)\text{O}_3$ -type perovskite materials, the B_1B_2 -site ion has a stronger effect on the refined energy level than that of A-site, which indicates that different composition of PMN can cause the distinct trend of OBG. For the PMN-PT single crystals, the OBG energy and domain wall scattering are the main contributions to optical loss, the mechanisms of which become increasingly important for the photon energies near the band gap. The BO_6 (TiO_6 , NbO_6 , and MgO_6) octahedron building block determines the basic energy level of the PMN-PT single crystals. The B-cation d orbitals associated with its octahedron govern the lower lying conduction bands and while the O-anion $2p$ orbitals and its octahedron rule the upper valence bands. Other ions in the structure contribute to

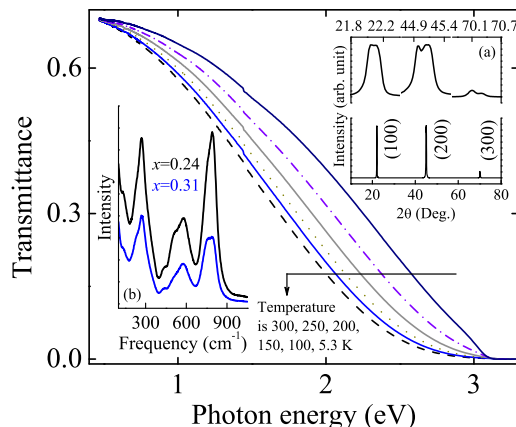


FIG. 2. (Color online) Transmittance spectra for the $\text{Pb}(\text{Mg}_{1/3}\text{Nb}_{2/3})\text{O}_3 - 0.31\text{PbTiO}_3$ (PMN-0.31PT) single crystal at the temperatures of 5.3 K, 100 K, 150 K, 200 K, 250 K, and 300 K, respectively. The inset (a) shows XRD pattern of the PMN-0.31PT single crystal at room temperature. The inset (b) shows Raman spectra for the PMN-0.24PT and PMN-0.31PT single crystals recorded at room temperature.

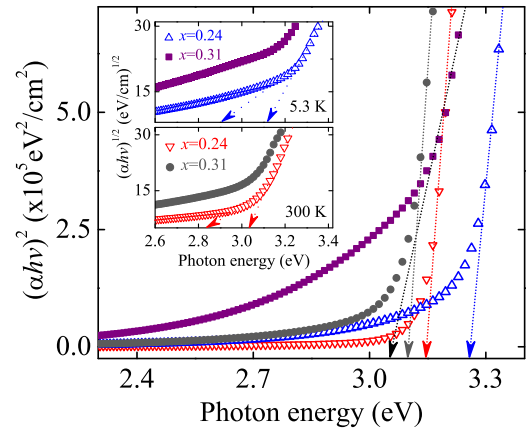


FIG. 3. (Color online) The variations in $(\alpha hv)^2$ with the photon energy for the PMN-0.24PT and PMN-0.31PT single crystals measured at 5.3 and 300 K. The inset shows the variations in $(\alpha hv)^{1/2}$ vs photon energy for the PMN-0.24PT and PMN-0.31PT crystals at 5.3 K and 300 K, respectively.

the higher-lying conduction band and have small effects. The dispersion behaviors of the PMN-PT single crystals, whose three types of ions occupy the same lattice position, are similar to most of ABO_3 -type perovskite compounds.⁶ It was reported that the density of PMN-PT has a slight increase with increasing PT composition. Furthermore, the $(\text{B}_1\text{B}_2)\text{O}_6$ -octahedra structure has more significant effect on the optical properties of crystal than the A-site ions.¹⁸

The fundamental interband transitions of the PMN-PT crystals include both direct and indirect transitions. According to the Fermi's golden rule, the absorption rate is proportional to the joint density of states in the allowed direct transition. For $h\nu \geq E_g$, $\alpha hv \propto (h\nu - E_{gd})^{1/2}$, where α is the absorption coefficient and E_{gd} is the allowed direct band gap. Unlike direct transition, indirect transition must contain a large change in the electron wave vector, which means that it involves the phonon to conserve momentum. The results of the quantum mechanical transition rate for an indirect transition can be expressed as $\alpha hv \propto (h\nu - E_{gi} \mp E_p)^2$, where E_{gi} is the indirect band gap and E_p is the energy of the phonon absorption (+) or emission (-). The plot of the $(\alpha hv)^2$ and $(\alpha hv)^{1/2}$ versus photon energy for the PMN-0.24PT and PMN-0.31PT crystals are shown in Fig. 3 and its inset, respectively. The values of E_{gd} , $E_{g1} = E_{gi} + E_p$, and $E_{g2} = E_{gi} - E_p$ can be obtained for the PMN-0.24PT crystal and E_{gd} for the PMN-0.31PT crystal by extrapolating the linear portion of the curves to zero, respectively. The phonon energy E_p of the PMN-0.24PT crystal is estimated to about 0.098 ± 0.014 eV (790 ± 113 cm^{-1}), which agrees well with the value (791 cm^{-1}) recorded by Raman spectra, as seen in the inset of Fig. 2. The phonon around 791 cm^{-1} corresponding to the Nb-O-Mg bond stretching mode, which is sensitive to the distortion of the BO_6 octahedra, plays an important role in the indirect transition. Note that the indirect band gap of the PMN-0.24PT crystal increases while the phonon frequency is almost invariable with decreasing the temperature, demonstrating a characteristic first-order behavior. It was confirmed by polarized Raman study of the phonon dynamics from 100 to 1000 K.¹⁹ The distortions in the form of lower symmetry clusters exist in the PMN-PT crystal because the first-order scattering is prohibited in the perfect cubic crystal. It was reported that the rhombohedral PMN-0.24PT crystal has different Raman active mode with the

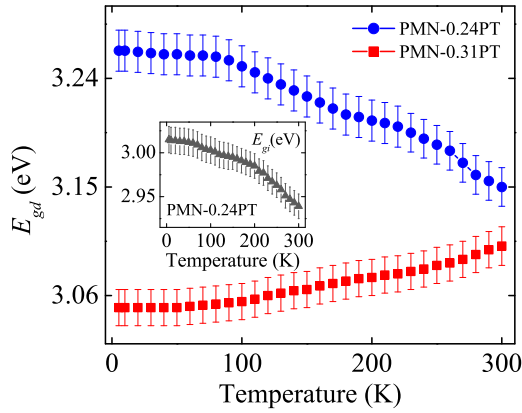


FIG. 4. (Color online) The direct band gaps of the PMN-0.24PT and PMN-0.31PT crystals are varied with the temperature. The inset shows that the indirect band gap of the PMN-0.24PT crystal decreases with the temperature.

PMN-0.31PT crystal.²⁰ The random fields, which induce the ordered polar nanoregions with negative charge, prevent the growth of the long range FE order. The PT addition is in favor of the long range order while the influence of ordered polar nanoregions remains powerful for the PMN-PT crystal even with small compositions of PT.

As shown in Fig. 4, the direct band gap of the PMN-0.24PT single crystal is slightly larger than that of the PMN-0.31PT single crystal, which reveals that the E_{gd} of the PMN-PT crystals show a redshift trend with increasing PT composition.⁷ It may be due to a larger band gap of pure PT crystal as compared to that of PMN. Similar phenomena have been observed in the PZNT crystals.²¹ With increasing the temperature, the direct band gap of the PMN-0.24PT crystal decreases from 3.263 ± 0.017 to 3.150 ± 0.016 eV while that of the PMN-0.31PT crystal increases from 3.050 ± 0.015 to 3.101 ± 0.016 eV, which may be due to a long-range coexistence symmetry evolution from the rhombohedral to monoclinic phase.¹² The monoclinic domains increase with the temperature at the expense of the rhombohedral domains. Similar phenomena about the tetragonal and monoclinic domain coexisting at low temperature were also observed in $\text{Pb}(\text{In}_{1/2}\text{Nb}_{1/2})\text{O}_3\text{-PbTiO}_3$ single crystal.^{1,22} The development of polar nanoclusters, which incorporate into the macroscopic FE domains, can cause a rapid decline of the OBG due to the increase in domain boundaries.²² The peculiar characteristic is mainly due to the multiphase coexistence of the PMN-0.31PT crystal over a wide temperature. Moreover, the indirect band gap E_{gi} of the PMN-0.24PT crystal, whose variation is smaller than that of the direct band gap E_{gd} , decreases from 3.015 ± 0.015 to 2.939 ± 0.014 eV with the temperature.

In $\text{Pb}(\text{B}_1\text{B}_2)\text{O}_3$ relaxorlike FE, the nanoregions, domain structure, and B_1B_2 -site cation structure mainly affect the OBG as well as the dielectric and piezoelectric behavior of the crystals. The PMN-PT crystal has a complex energy distribution, where Mg^{2+} , Nb^{5+} , and Ti^{4+} ions occupy the same crystallographic site in the structure. The distortion of lattice, ion vibration and interaction of the ions with different poling direction comprises the complex mechanism to reveal the electronic structures.¹⁸ The structure of the PMN-PT single crystal consists of the BO_6 polyhedra, including NbO_6 ,

MgO_6 , and TiO_6 octahedra. The TiO_6 octahedra are pressed by the NbO_6 and MgO_6 , causing the latter two distorting along the $\langle 001 \rangle$ direction. When decreasing the temperature, NbO_6 and MgO_6 octahedra slip the leash of TiO_6 octahedra distort along $\langle 111 \rangle$, resulting in the long-range increasing fraction of coexistence from the monoclinic to rhombohedral transition.

In conclusion, we have investigated the optical properties of (001)-face PMN-PT single crystals. It was found that the direct band gap of the PMN-0.24PT crystal has a negative temperature coefficient while the PMN-0.31PT crystal has a positive variation. The multiphase coexistence in the PMN-0.31PT crystal over a wide temperature range, which is associated with M_C type monoclinic phase, can explain the abnormal optical properties.

This work was supported by NSFC (Grant Nos. 60906046 and 11074076), Major State Basic Research Development Program of China (Grant Nos. 2007CB924901 and 2011CB922200), Program of NCET, MOE (Grant No. NCET-08-0192), STCSM Project (Grant Nos. 10DJ1400201, 10SG28, 10ZR1409800, and 09ZZ42), the High Technology and Development Project of China (Grant No. 2008AA03Z411), and the Program for Professor of Special Appointment (Eastern Scholar) at Shanghai Institutions of Higher Learning.

¹S. E. Park and T. R. Shrout, *J. Appl. Phys.* **82**, 1804 (1997).

²G. S. Xu, X. F. Wang, D. F. Yang, Z. Q. Duan, C. D. Feng, and K. Chen, *Appl. Phys. Lett.* **86**, 032902 (2005).

³G. S. Xu, H. S. Luo, H. Q. Xu, and Z. W. Yin, *Phys. Rev. B* **64**, 020102(R) (2001).

⁴Z. G. Hu, Y. W. Li, F. Y. Yue, Z. Q. Zhu, and J. H. Chu, *Appl. Phys. Lett.* **91**, 221903 (2007).

⁵W. W. Li, J. J. Zhu, J. D. Wu, J. Gan, Z. G. Hu, M. Zhu, and J. H. Chu, *Appl. Phys. Lett.* **97**, 121102 (2010).

⁶C. J. He, L. H. Luo, X. Y. Zhao, H. Q. Xu, X. H. Zhang, T. H. He, H. S. Luo, and Z. X. Zhou, *J. Appl. Phys.* **100**, 013112 (2006).

⁷K. Y. Chan, W. S. Tang, C. L. Mak, and K. H. Wong, *Phys. Rev. B* **69**, 144111 (2004).

⁸A. K. Singh and D. Pandey, *Phys. Rev. B* **67**, 064102 (2003).

⁹Z. G. Ye, B. Noheda, M. Dong, D. E. Cox, and G. Shirane, *Phys. Rev. B* **64**, 184114 (2001).

¹⁰J. M. Kiat, Y. Uesu, B. Dkhil, M. Matsuda, C. Malibert, and G. Calvarin, *Phys. Rev. B* **65**, 064106 (2002).

¹¹S. P. Singh, S. Yoon, S. Baik, N. Shin, and D. Pandey, *Appl. Phys. Lett.* **97**, 122902 (2010).

¹²R. R. Chien, V. H. Schmidt, L. W. Hung, and C. S. Tu, *J. Appl. Phys.* **97**, 114112 (2005).

¹³B. Noheda, D. E. Cox, G. Shirane, J. A. Gonzalo, L. E. Cross, and S. E. Park, *Appl. Phys. Lett.* **74**, 2059 (1999).

¹⁴W. S. Chang, L. C. Lim, P. Yang, C. S. Ku, H. Y. Lee, and C. S. Tu, *J. Appl. Phys.* **108**, 044105 (2010).

¹⁵R. Guo, L. E. Cross, S. E. Park, B. Noheda, D. E. Cox, and G. Shirane, *Phys. Rev. Lett.* **84**, 5423 (2000).

¹⁶B. Noheda, D. E. Cox, G. Shirane, J. Gao, and Z. G. Ye, *Phys. Rev. B* **66**, 054104 (2002).

¹⁷B. Noheda, Z. Zhong, D. E. Cox, G. Shirane, S. E. Park, and P. Pehrig, *Phys. Rev. B* **65**, 224101 (2002).

¹⁸Y. H. Bing, R. Guo, and A. S. Bhalla, *Ferroelectrics* **242**, 1 (2000).

¹⁹O. Svitelskiy, J. Toulouse, G. Yong, and Z. G. Ye, *Phys. Rev. B* **68**, 104107 (2003).

²⁰Y. Yang, Y. L. Liu, L. Y. Zhang, K. Zhu, S. Y. Ma, G. G. Siu, Z. K. Xu, and H. S. Luo, *J. Raman Spectrosc.* **41**, 1735 (2010).

²¹E. Sun, R. Zhang, Z. Wang, D. Xu, L. Li, and W. Cao, *J. Appl. Phys.* **107**, 113532 (2010).

²²C. S. Tu, F. T. Wang, C. M. Hung, R. R. Chien, and H. S. Luo, *J. Appl. Phys.* **100**, 104104 (2006).